

Faddeev calculations for the ${}^9_{\Lambda}\text{Be}$ spectrum

I. Filikhin^{1,a}, V. M. Suslov^{1,2} and B. Vlahovic¹

¹ North Carolina Central University, Durham, NC, 27707, USA

² Saint-Petersburg State University, Petrodvorets, St. Petersburg, Russia

Abstract. An α -cluster model is applied to study low-lying spectrum of the ${}^9_{\Lambda}\text{Be}$ hypernucleus. The $\alpha\alpha\Lambda$ three-body problem is numerically solved by the Faddeev equations in configuration space using phenomenological pair potentials. Found is a set of the potentials that reproduces experimental data for the ground state ($\frac{1}{2}^+$) binding energy and excitation energy of the $\frac{5}{2}^+$ and $\frac{3}{2}^+$ states, simultaneously. This set includes the Ali-Bodmer potential of version "e" for $\alpha\alpha$ and modified Tang-Herdon potential for $\alpha\Lambda$ interactions. The spin-orbit $\alpha\Lambda$ interaction is given by modified Scheerbaum potential. Low-lying energy levels are evaluated applying a variant of the analytical continuation method in coupling constant, and the experimental data for excitation energies are well reproduced by our calculations. This result improves previous α -cluster calculations. It is shown that the spectral properties of ${}^9_{\Lambda}\text{Be}$ can be classified as an analog of ${}^9\text{Be}$ spectrum with the exception of several "genuine hypernuclear states", which agrees qualitatively with previous studies. The energy splitting of spin-flip doublet ($\frac{9}{2}^+$, $\frac{7}{2}^+$) is predicted.

1 Introduction

Long time interest to the ${}^9_{\Lambda}\text{Be}$ hypernucleus can be explained by usefully applying this system in the hyperon-nucleon interaction studies (in particular, for the spin-orbit component of this interaction) [1–5].

The clear cluster structure of this nucleus allows to apply well established few-body physics methods. The bound states have been studied within the $\alpha + \alpha + \Lambda$ model in a number of works [2,3,5–12]. Nevertheless, theoretical studies for resonance states of ${}^9_{\Lambda}\text{Be}$ in the cluster model are limited by qualitative description of the ${}^9_{\Lambda}\text{Be}$ spectrum [3,13–15]. In particular, a classification of the resonance states, including "genuine" hypernuclear states [3], is presented.

In the present work we renew the theoretical results [16] for energy of the ${}^9_{\Lambda}\text{Be}$ resonances using the $\alpha + \alpha + \Lambda$ cluster model. Mathematical basis of our calculations are the configuration space Faddeev equations [17].

For description of $\alpha\alpha$ nuclear interaction the Ali - Bodmer potential [18] is used. This potential with s , d and g -wave components has strong repulsive s -wave core that simulates the Pauli blocking for two α particles. To reach better agreement with experimental data we considered three modifications of this potential. For the $\alpha\Lambda$ potential a type of coordinate dependence is uncertain. The $\alpha\Lambda$ experimental data are limited by the value of the binding energy of the ${}^5_{\Lambda}\text{He}$ hypernucleus, which is considered as the bound s -wave state of the $\alpha\Lambda$ system. In our calculations, several phenomenological models are applied for the central part

of $\alpha\Lambda$ interaction. A new model motivated by the Tang-Herdon potential [19] is proposed in present work. Also we have focused on the spin-orbit component of $\alpha\Lambda$ interaction. We adjusted the parameters of the $\alpha\Lambda$ spin-orbit potential known from literature [5] to construct the model that reproduces experimental data for the ground state ($\frac{1}{2}^+$) binding energy and excitation energy of the $\frac{5}{2}^+$ and $\frac{3}{2}^+$ states, simultaneously. Note that in our model the central part (s -wave) of $\alpha\Lambda$ interaction is used for all partial waves of the pair $\alpha\Lambda$ (see alternative models in [10,20]). Based on the model we predicted the energy spacing of spin-flip doublet ($\frac{9}{2}^+$, $\frac{7}{2}^+$).

Additionally our model well reproduces the experimental data for excitation energies of ${}^9_{\Lambda}\text{Be}$ low-lying levels. Thus new classification for peaks measured in the (π^+ , K^+) experiments [16] is given. This result improves previous calculations of the ${}^9_{\Lambda}\text{Be}$ spectrum [14]. It is shown that the spectral properties of ${}^9_{\Lambda}\text{Be}$ can be classified as an analog of ${}^9\text{Be}$ spectrum with the exception of several "genuine hypernuclear states". This agrees qualitatively with previous studies [2,3,21].

2 Formalism

The Faddeev equations in coordinate space [17] are used for description of the ${}^9_{\Lambda}\text{Be}$ hypernucleus, considered as a three-body $\alpha\alpha\Lambda$ system. General form of the equations is as follows:

$$\{H_0 + V_{\gamma}^s(|\mathbf{x}_{\gamma}|) + \sum_{\beta=1}^3 V_{\beta}^{Coul.}(|\mathbf{x}_{\beta}|) - E\} \Psi_{\gamma}(\mathbf{x}_{\gamma}, \mathbf{y}_{\gamma}) =$$

^a e-mail: ifilikhin@nccu.edu

$$= -V_\gamma^s(|\mathbf{x}_\gamma|) \sum_{\beta \neq \gamma} \Psi_\beta(\mathbf{x}_\beta, \mathbf{y}_\beta),$$

here $V_\beta^{Coul.}$ is the Coulomb potential between the particles belonging to the pair β , and V_γ^s is the short-range pair potential in the channel γ , ($\gamma=1,2,3$). $H_0 = -\Delta_{\mathbf{x}_\gamma} - \Delta_{\mathbf{y}_\gamma}$ is the kinetic energy operator, E is the total energy and Ψ - the wave function of the three-body system. Ψ is given as a sum over three Faddeev components, $\Psi = \sum_{\gamma=1}^3 \Psi_\gamma$. For the $\alpha\alpha\Lambda$ system including two identical particles the coupled set of the Faddeev equations is written as:

$$\begin{aligned} (H_0 + V_{\alpha\Lambda}^s + V^{Coul.} - E)W &= -V_{\alpha\Lambda}^s (U + P_{12}W), \\ (H_0 + V_{\alpha\alpha}^s + V^{Coul.} - E)U &= -V_{\alpha\alpha}^s (W + P_{12}W), \end{aligned} \quad (1)$$

where P_{12} is the permutation operator for the α particles (particles 1,2), $V_{\alpha\alpha}^s$ and $V_{\alpha\Lambda}^s$ are nuclear potentials of $\alpha\alpha$ and $\alpha\Lambda$ interactions, respectively. $V^{Coul.}$ is the potential of Coulomb interaction between the α particles, U is the Faddeev component corresponding to the rearrangement channel ($\alpha\alpha$) - Λ and W corresponds to the rearrangement channel ($\alpha\Lambda$) - α . The total wave function is expressed by the components U and W with relation $\Psi = U + (1 + P_{12})W$. The total orbital angular momentum is given by $\mathbf{L} = \ell_{\alpha\alpha} + \lambda_{(\alpha\alpha)-\Lambda} = \ell_{\alpha\Lambda} + \lambda_{(\alpha\Lambda)-\alpha}$, where $\ell_{\alpha\alpha}$ ($\ell_{\alpha\Lambda}$) is the orbital angular momentum of α 's (pair of $\alpha\Lambda$) and $\lambda_{(\alpha\alpha)-\Lambda}$ ($\lambda_{(\alpha\Lambda)-\alpha}$) is the orbital angular momentum of a Λ hyperon (α particle) relatively to the center of mass of the pair α ($\alpha\Lambda$) particles.

Possible combinations for relative momenta $\ell_{\alpha\alpha}$, $\lambda_{(\alpha\alpha)-\Lambda}$ and $\ell_{\alpha\Lambda}$, $\lambda_{(\alpha\Lambda)-\alpha}$ written as a block have form:

$$\begin{pmatrix} \{ \ell_{\alpha\Lambda} \} \\ \{ \lambda_{(\alpha\Lambda)-\alpha} \} \end{pmatrix} \begin{pmatrix} \{ \ell_{\alpha\alpha} \} \\ \{ \lambda_{(\alpha\alpha)-\Lambda} \} \end{pmatrix},$$

where each block represents all quantum numbers taken into account. For example the combinations corresponding the 0^+ state are:

$$\begin{pmatrix} \{ \ell_{\alpha\Lambda} \} \\ \{ \lambda_{(\alpha\Lambda)-\alpha} \} \end{pmatrix} \begin{pmatrix} \{ \ell_{\alpha\alpha} \} \\ \{ \lambda_{(\alpha\alpha)-\Lambda} \} \end{pmatrix} = \begin{pmatrix} 0 & 1 & 2 & \dots \end{pmatrix} \begin{pmatrix} 0 & 2 & 4 & \dots \end{pmatrix}.$$

The ground state of the $\alpha\alpha\Lambda$ system, having zero total angular momentum L , is considered as the $(\frac{1}{2})^+$ state of the ${}^9_\Lambda\text{Be}$ hypernucleus.

More detail description of this formalism is given in Ref. [10], where the particles of the $\alpha\alpha\Lambda$ system interact only by local pairwise central potentials. In the present paper the spin-orbital component of the $\alpha\Lambda$ interaction is taken into account. Thus the $\alpha\Lambda$ potential is written as a sum of central and spin-orbit parts: $V_{\alpha\Lambda}^s = V_{\alpha\Lambda}^c + V_{\alpha\Lambda}^{so}$. In the LS basis the matrix elements of the spin-orbital potential $V_{\alpha\Lambda}^{so}$ are given by the following form:

$$\begin{aligned} V_{\alpha\Lambda}^{so}(r) &= \frac{2L+1}{2} \sum_{j=l\pm 1/2} (2j+1) \left\{ \begin{matrix} J & L & 1/2 \\ l & j & \lambda \end{matrix} \right\}^2 \\ &\times (j(j+1) - l(l+1) - 3/4)v_{so}(r), \end{aligned} \quad (2)$$

where J is the total three-body angular momentum, L is the total three-body orbital momentum, j , and l are total

orbital momenta of the $\alpha\Lambda$ pair (spin of the pair is equal to $\frac{1}{2}$), λ is orbital momentum of α -particle with respect to the center of the $\alpha\Lambda$ pair, and $v_{so}(r)$ is a coordinate part of the $\alpha\Lambda$ spin-orbit potential. In the LS basis the $\alpha\Lambda$ potential is represented by diagonal matrix with diagonal elements: $V_{\alpha\Lambda}^s(r) = v_c^l(r) + V_{\alpha\Lambda}^{so}(r)$, where $v_c^l(r)$ is central l -partial component of the $\alpha\Lambda$ potential.

3 Potentials

For description of the central part of the $\alpha\Lambda$ interaction, phenomenological potentials are used. The Gibson [22] and Tang-Herndon (TH) [19] potentials have the form of one range Gaussian and are fully attractive:

$$v_c(r) = -V_c \exp(-\alpha_c r^2).$$

The range V_c and strength α_c parameters of these potentials are listed in Tabl. 1.

The Isle potential [23] has two range Gaussian form with weak repulsive core. These potentials reproduce well experimental value of the binding energy for the ${}^5_\Lambda\text{He}$ hypernucleus, which is considered as an s -wave bound state of the $\alpha\Lambda$ system with energy of 3.12 ± 0.02 MeV. For the $\alpha\alpha\Lambda$ calculations we assume that the central s -wave $\alpha\Lambda$ potential acts in all partial waves of the $\alpha\Lambda$ subsystem.

For the spin-orbit part of the $\alpha\Lambda$ interaction there are several models [4,5] and we used one that simulates the Scheerbaum (S) potential [5]. Our fit for the potential is given by one range Gaussian form:

$$v_{so}(r) = V_{so} \exp(-\alpha_{so} r^2). \quad (3)$$

Here $V_{so} = -9$ MeV is the strength parameter and $\alpha_{so} = 0.3241$ fm $^{-2}$ is the range parameter. The models [4,5] of the $\alpha\Lambda$ spin-orbit interaction overestimate the experimental value of the doublet spin orbit splitting of the $\frac{5}{2}^+$ and $\frac{3}{2}^+$ states of ${}^9_\Lambda\text{Be}$. In Ref. [24] the experimental value for ($\frac{5}{2}^+$, $\frac{3}{2}^+$) energy splitting is explained by taking into account the $\Lambda N \rightarrow \Sigma N$ coupling effect. In this work we restrict ourselves by a model without the $\Lambda N \rightarrow \Sigma N$ conversion. It is assumed that this effect is small and that it can be effectively taken into account by phenomenological $\alpha\Lambda$ potential.

Nuclear $\alpha\alpha$ interaction is given by the phenomenological Ali-Bodmer (AB) potential [18]. This potential has the following form: $V_{\alpha\alpha}(r) = \sum_{l=0,2,4} V_{\alpha\alpha}^l(r) P_l$, where P_l is a projector onto the state of the $\alpha\alpha$ pair with the orbital momentum l . The functions $V_{\alpha\alpha}^l(r)$ have the form of one or two range Gaussians:

$$V_{\alpha\alpha}^l(r) = V_{rep}^l \exp(-\beta_{rep}^l r^2) - V_{att}^l \exp(-\beta_{att}^l r^2). \quad (4)$$

The s -wave component $V_{\alpha\alpha}^0(r)$ has a strong repulsive core which simulates Pauli blocking effect for the α 's at short distances. There are different sets of the parameters for partial components $V_{\alpha\alpha}^l(r)$ [18]. The parameters of version "e" of the Ali-Bodmer potential (ABe) are given in Table 1.

Table 1. Parameters of the $\alpha\alpha$ and $\alpha\Lambda$ potentials. The pair angular momentum is l . V_{att}^l (V_{rep}^l) and V_c are given in MeV, β_{att}^l (β_{rep}^l) in fm^{-1} and α_c in fm^{-2} .

| Interac. | Pot. | l | V_{rep}^l | β_{rep}^l | V_{att}^l | β_{att}^l |
|-----------------|-------------|-----|--------------------|------------------------|--------------------|------------------------|
| $\alpha\alpha$ | ABe [18] | 0 | 1050 | 0.8 | 150 | 0.5 |
| | | 2 | 640 | 0.8 | 150 | 0.5 |
| | | 4 | – | – | 150 | 0.5 |
| | | | V_c | | α_c | |
| $\alpha\Lambda$ | TH [19] | 0 | | | 60.17 | 0.6172 |
| | Gibson [22] | 0 | | | 43.48 | 0.4024 |

4 Methods

Bound state problem based on the configuration space Faddeev equations (1) for the $\alpha\alpha\Lambda$ system is solved numerically, applying the finite difference approximation with spline collocations [25, 10]. For calculation of the eigenvalues the method of inverse iterations is used. To estimate the energies and widths of low-lying resonance states we applied the method of analytical continuation in coupling constant [27]. A variant of this method with an additional non-physical three-body potential is used. The strength parameter of this potential is considered as variational parameter for analytical continuation of the bound state energy in complex plane [28–30]. This potential is considered as a perturbation to corresponding three body hamiltonian and is added to the left hand side of the equations (1). The three-body potential has the form: $V_3(\rho) = -\delta \exp(-b\rho^2)$. Parameters of this potential are $b=0.1 \text{ fm}^{-1}$ and $\delta \geq 0$ (variational parameter), $\rho^2 = x_\alpha^2 + y_\alpha^2$, where x_α, y_α are the mass scaled Jacobi coordinates ($\alpha = 1, 2$) [11]. For each resonance there exist a region $|\delta| \geq |\delta_0|$ where a resonance becomes a bound state. In this region we obtain $2N$ three-body bound state energies corresponding to $2N$ values of δ . The continuation of the energy into complex plane is carried out by means of the Padé approximation: $\sqrt{-E} = \frac{\sum_{i=1}^N p_i \xi^i}{1 + \sum_{i=1}^N q_i \xi^i}$ where $\xi = \sqrt{\delta_0 - \delta}$. The Padé approximation for $\delta = 0$ gives the energy and width of resonance: $E(\delta = 0) = E_r + i\Gamma/2$. Note that accuracy of the Padé interpolation for resonance energy and width decreases with increasing distance from the scattering threshold. Accuracy of the calculated resonance parameters can be evaluated by the differences of their values obtained for different orders N of the Padé approximants.

5 Calculations

5.1 Bound states

The ${}^9_\Lambda\text{Be}$ hypernucleus has two bound states: ground state with total angular momentum $L = 0$ (0^+ state) and excited state with $L = 2$ (2^+ state). The latter state is splitted into two states due to $\alpha\Lambda$ spin-orbit interaction. Total orbital momenta of these states are $\frac{1}{2}^+$, $\frac{3}{2}^+$ and $\frac{5}{2}^+$, respectively.

Subsystem momentum configuration for the 0^+ state may be restricted by the values:

$$\begin{aligned} (\ell_{\alpha\Lambda}) (\ell_{\alpha\alpha}) &= (0\ 1\ 2) (0\ 2\ 4) \\ (\lambda_{(\alpha\Lambda)-\alpha}) (\lambda_{(\alpha\alpha)-\Lambda}) &= (0\ 1\ 2) (0\ 2\ 4). \end{aligned}$$

It is well known that the s -wave component of the total wave function brings the main contribution to the energy of the state and for calculation of the binding energy one may take into account the first three partial waves in each channel [8, 10]. The configuration of the angular momenta corresponding to 2^+ state taken into account are:

$$\begin{aligned} (\ell_{\alpha\Lambda}) (\ell_{\alpha\alpha}) &= (0\ 1\ 1\ 2\ 2\ 2) (0\ 2\ 2\ 2\ 4\ 4) \\ (\lambda_{(\alpha\Lambda)-\alpha}) (\lambda_{(\alpha\alpha)-\Lambda}) &= (2\ 1\ 3\ 0\ 2\ 4) (2\ 0\ 2\ 4\ 2\ 4). \end{aligned}$$

This set of momenta provides convergence for binding energy with satisfactory accuracy, as it is found in [8, 9, 11, 10].

In Tabl. 2 calculated energies for the bound states of the $\alpha\alpha\Lambda$ system are presented. We used various potential models in these calculations. In particular three variants of the $\alpha\alpha$ Ali-Bodmer potential are used [18] (ABa, ABd, ABe). Note that the model "a*" of the ABA potential is modified in [31]. For the $\alpha\Lambda$ interaction we apply the TH, Gibson, and Isle potentials.

Detail comparison of the results of Faddeev calculation for the $\alpha\alpha\Lambda$ system with the Gibson (or TH) and Isle potential (ABa potential for the $\alpha\alpha$ interaction) one can find in [10]. The calculated energy of the ground state is close to the experimental emulsion data [32] for Gibson potential whereas the Isle potential overbinds the $\alpha\alpha\Lambda$ system for about 1.5 Mev. In [10] it is shown that this overbinding can be explained by two effects: first the Isle potential has the weak repulsive core which is absent for the Gibson potential. This difference leads to more space spreading of the wave function of the $\alpha\alpha\Lambda$ system calculated with the Isle potential in comparison with the Gibson (or TH) potential. In the compact $\alpha\alpha\Lambda$ system the repulsive core of the $\alpha\alpha$ potential gives smaller absolute value of the ground state energy (so called "core effect" in [10, 11]). The second results from the first: in a more compact $\alpha\alpha\Lambda$ system (with Gibson potential) the contributions of higher partial waves of $\alpha\Lambda$ potential in the energy is smaller. It may give smaller absolute value of the ground state energy for the Gibson (or TH) potential.

As it is found in [10] the energy contribution of the p -wave component of the Isle $\alpha\Lambda$ potential is unnaturally large and results obtained for energy of the bound states are too large in absolute value, compared with experimental data. For Gibson potential one can see from Tabl. 2 that agreement with data is good. However, it is shown in Ref. [15] that application of the combination of the ABA+Gibson potentials for calculation of ground band levels of the $\alpha\alpha\Lambda$ system leads to appearance of the additional virtual states and resonances, which have not been found in previous studies [16]. Localization of the state on energy scale is obtained to be in clear disagreement with the experimental picture.

We modified the TH potential parameters V_c and α_c to be 54.36 MeV and 0.538 fm^{-2} , respectively, this model

Table 2. Binding energy E_B (in MeV) and excited energy E_x (in MeV) of degenerate $(3/2^+, 5/2^+)$ spin doublet state of the $\alpha\alpha\Lambda$ system for different models of the $\alpha\alpha$ and $\alpha\Lambda$ interactions. The energy of spin-flip doublet splitting ΔE (in keV) is given for the Scheerbaum (S) potential from Ref. [5] ($V_{so}=-9$ MeV, $\alpha_{so}=0.3241$ fm $^{-2}$). Modification S(M) of the spin-orbit potential is made by changing the α parameter to be similar to $\alpha\Lambda$ potential. Energy is measured from the $\alpha + \alpha + \Lambda$ threshold. Orbital quantum numbers are $\{l_{\alpha\Lambda}\}=0,1,2$, $\{l_{\alpha\alpha}\}=0,2,4$ for the ground state and $\{l_{\alpha\Lambda}\} \leq 2$, $\{l_{\alpha\alpha}\} \leq 4$ for the excited states. The experimental data are taken from [26, 16].

| | AB | TH | TH(M) | Gibson | Isle | Exp. |
|--------------------|----|--------|--------|--------|--------|-------|
| E_B | a* | -5.990 | – | -6.709 | -8.119 | -6.62 |
| | d | -5.994 | – | -6.751 | -8.348 | |
| | e | -6.280 | -6.602 | -7.073 | -8.714 | |
| E_x | a* | 2.562 | – | 2.621 | 2.902 | 3.04 |
| | d | 2.738 | – | 2.756 | 2.927 | |
| | e | 2.990 | 2.99 | 3.032 | 3.193 | |
| ΔE | a* | 450 | – | 509 | 511 | 43 |
| | S | d | 346 | – | 447 | 512 |
| | e | 352 | 378 | 457 | 525 | |
| ΔE S(M) | e | 126 | 172 | – | – | |

* $a_0 a_2 d_4$.

is denoted as TH(M). One can see that the TH(M) model together with the ABe potential leads to good reproduction of the experimental data for ${}^9_\Lambda\text{Be}$ bound states.

The energy of spin-flip doublet splitting ΔE is calculated for the potential S [5] ($\alpha_{so}=0.3241$ fm $^{-2}$) and for its modified version S(M). In the first case we have very large values for the energy splitting, if compared by the experimental data. This disagreement may be decreased by a modification of the spin-orbit potential motivated by assumption that the range parameter of this potential should be similar to the range of the central part (see also Tabl. 1). After this modification the energy of the spin-orbit splitting (TH(M) + ABe + S(M) model) is decreased to the value that is comparable to the results of previous calculations: 160 keV [4] and 147 keV [5].

Our next modification of the spin-orbit potential S(M) is performed by adjusting strength parameter V_{so} . The experimental value of 43(5) keV [26] is reproduced by our calculation using for $V_{so}=2.25$ MeV (this value of V_{so} is three times smaller than initial value (the S potential)). The excitation energy for the doublet members is 3.016 MeV ($\frac{3}{2}^+$) and 2.972 MeV ($\frac{5}{2}^+$). The state $\frac{3}{2}^+$ is upper member of this doublet, which agrees with previous calculation [21]. Keeping this value for the strength parameter V_{so} we evaluated the energy spacing of other spin-flip doublet ($\frac{7}{2}^+$, $\frac{9}{2}^+$) that has orbital momentum 4^+ . Our prediction for this energy is 200 keV and upper member of the doublet is the state $\frac{7}{2}^+$.

5.2 Resonances

For calculation of the energy of the resonance states a variant of the method of analytical continuation in coupling constant is applied [27]. We changed the coupling constant δ of an additional three-body potential (1) to construct the analytical continuation of negative bound state energy, dependent on δ , in complex plane. The energy of resonance is calculated using the Pade extrapolation (as function of δ) to the point with $\delta=0$.

The configurations of the angular momenta corresponding to the L^x states which we took into account are shown below:

4⁺ states

$$\begin{pmatrix} \ell_{\alpha\Lambda} \\ \lambda_{(\alpha\Lambda)-\alpha} \end{pmatrix} \begin{pmatrix} \ell_{\alpha\alpha} \\ \lambda_{(\alpha\alpha)-\Lambda} \end{pmatrix} = (0\ 1\ 2\ 2\ 3\ 4) (0\ 2\ 4\ 2\ 4) \\ = (4\ 3\ 2\ 4\ 1\ 0) (4\ 2\ 2\ 4\ 0)$$

2⁻ state

$$\begin{pmatrix} \ell_{\alpha\Lambda} \\ \lambda_{(\alpha\Lambda)-\alpha} \end{pmatrix} \begin{pmatrix} \ell_{\alpha\alpha} \\ \lambda_{(\alpha\alpha)-\Lambda} \end{pmatrix} = (1\ 2\ 2\ 3\ 3\ 4) (2\ 2\ 4) \\ = (2\ 1\ 3\ 2\ 4\ 3) (1\ 3\ 3)$$

4⁻ state

$$\begin{pmatrix} \ell_{\alpha\Lambda} \\ \lambda_{(\alpha\Lambda)-\alpha} \end{pmatrix} \begin{pmatrix} \ell_{\alpha\alpha} \\ \lambda_{(\alpha\alpha)-\Lambda} \end{pmatrix} = (1\ 2\ 2\ 3\ 4\ 4) (2\ 2\ 4\ 4) \\ = (4\ 3\ 5\ 2\ 1\ 3) (3\ 5\ 1\ 3)$$

3⁻ state

$$\begin{pmatrix} \ell_{\alpha\Lambda} \\ \lambda_{(\alpha\Lambda)-\alpha} \end{pmatrix} \begin{pmatrix} \ell_{\alpha\alpha} \\ \lambda_{(\alpha\alpha)-\Lambda} \end{pmatrix} = (0\ 3\ 2\ 1\ 1\ 4) (0\ 2\ 2\ 4\ 4) \\ = (3\ 0\ 1\ 2\ 4\ 1) (3\ 1\ 3\ 1\ 3)$$

5⁻ state

$$\begin{pmatrix} \ell_{\alpha\Lambda} \\ \lambda_{(\alpha\Lambda)-\alpha} \end{pmatrix} \begin{pmatrix} \ell_{\alpha\alpha} \\ \lambda_{(\alpha\alpha)-\Lambda} \end{pmatrix} = (0\ 1\ 2\ 3\ 4\ 5) (0\ 2\ 2\ 4) \\ = (5\ 4\ 3\ 2\ 1\ 0) (5\ 3\ 5\ 1)$$

1⁻ state

$$\begin{pmatrix} \ell_{\alpha\Lambda} \\ \lambda_{(\alpha\Lambda)-\alpha} \end{pmatrix} \begin{pmatrix} \ell_{\alpha\alpha} \\ \lambda_{(\alpha\alpha)-\Lambda} \end{pmatrix} = (0\ 1\ 1\ 2\ 2\ 3) (0\ 2\ 2\ 2\ 4) \\ = (1\ 0\ 2\ 1\ 3\ 2) (1\ 1\ 3\ 3\ 5)$$

Following [3, 2] one may associate "ground band" the states with orbital momenta 0^+ , 2^+ and 4^+ . This band is connected with the ground band of ${}^8\text{Be}$ nucleus. In particular the 0^+ (ground state of ${}^8\text{Be}$), 2^+ and 4^+ states of ${}^8\text{Be}$ correspond to the "ground band" of ${}^9_\Lambda\text{Be}$ with the same excitation energies. The "glue-like" role of the Λ hyperon is followed by the fact that all ground band states of ${}^8\text{Be}$ are resonances, since the 0^+ and 2^+ states are bound states. As we will see further the "glue-like" effect of Λ -hyperon is stronger for the states of ${}^9_\Lambda\text{Be}$ with negative parity. The strong repulsive character of the $\alpha\alpha$ interaction in s -wave decreases the "glue-like" effect for "ground band" states where the s -wave has important contribution. For the states with negative parity this repulsive contribution is smaller. For example, in the state 2^- and 4^- there is no the s -wave of the $\alpha\alpha$ potential (see combinations of momenta in the $\Lambda\alpha\alpha$ system, above).

In Tabl. 3 are shown experimental data for ${}^9_\Lambda\text{Be}$ spectrum along with the results of our calculations. One can see that the resonance obtained in our calculations correspond

Table 3. Excitation energies E_x (in MeV) of low-lying states of $\alpha\alpha\Lambda$ system. Energies of peaks measured in the (π^+, K^+) experiments are given from [16].

| Exp. [16] | ABe+TH(M)+S(MM) model | L^π | J^π |
|------------------|-----------------------|---------|---------|
| 2.93 or 3.04 | 2.918 | 2^+ | 2^+ |
| 5.80 ± 0.13 | 5.7(1) | 1_1^- | 1_1^- |
| 9.52 ± 0.13 | 8.5(0) | 4^+ | 4^+ |
| 14.88 ± 0.10 | 14.(7) | 3_1^- | 3_1^- |
| 17.13 ± 0.20 | 17.(6) | 1_2^- | 1_2^- |
| 19.54 ± 0.32 | 21.(3) | 2^- | 2^- |
| 23.40 ± 0.21 | 23.(0) | 3_2^- | 3_2^- |

to the energies of the peaks measured in the (π^+, K^+) experiments [16] with good accuracy. Thus we give a new classification for the experimental data. Previous attempt for this classification is presented in Fig. 1 by results of cluster calculation [14, 16]. These results demonstrate essential disagreement with the experiment (except the bound states).

Our results are in good agreement with experiments for both bound states and resonances. Note that we neglect the spin-orbit splittings in this calculations due to their small energy spacings relative to energy differences between states with different orbital numbers.

Finally we give comparison between the ${}^9_\Lambda\text{Be}$ (calculated) and ${}^9\text{Be}$ (experimental) spectra in Fig. 2. This comparison could help to define the "genuine hypernuclear states" [3] of ${}^9_\Lambda\text{Be}$. Connections between states with equal orbital momentum denoted by the fine lines in Fig. 2 indicate that there are two ${}^9_\Lambda\text{Be}$ states that have no analogs in the ${}^9\text{Be}$ spectrum. These states with orbital momenta 1^- and 3^- are "genuine hypernuclear states". This conclusion is in qualitative agreement with previous studies [16]. As we showed above the localization of these states on energy scale is different from those reported in [16].

5.3 Three-body potential for $\alpha\alpha\Lambda$ system

Treatment of an α -cluster model [12] (see also [33]) for ${}^9_\Lambda\text{Be}$ includes a three-body $\alpha\alpha\Lambda$ potential which due to the NNA interaction exists in the nuclear system as it is explained in [12]. With the $\alpha\alpha\Lambda$ potential presented in [12] one can obtain satisfactory results for the 0^+ binding energy and excitation energy of the 2^+ state while the Ali-Bodmer potential of the version "a" is chosen for $\alpha\alpha$ interaction and the Isle [23] (or MSA [20]) potential is chosen for $\alpha\Lambda$ interaction. Note that the three-body potential [12] is repulsive. Thus the overbinding problem [10] of the $\alpha\alpha\Lambda$ system with the Isle (MSA) $\alpha\Lambda$ potential can be solved by including the three-body potential into the consideration. At the same time for the $\alpha\Lambda$ potentials similar to Gibson or TH, which bind the $\alpha\alpha\Lambda$ system weaker than it follows from ${}^9_\Lambda\text{Be}$ experiment, perhaps the three-body potential has to have attractive character.

The calculated binding energy E_B of ground state and the first excited ($3/2^+$, $5/2^+$) states are presented in Tabl.

Table 4. Calculated binding energy E_B (in MeV) of ground state and first excited ($3/2^+$, $5/2^+$) states for the $\alpha\alpha\Lambda$ system. Excitation energy E_x is calculated with no spin-orbit interaction. All notations are the same as in Table 1. The three-body $\alpha\alpha\Lambda$ potential given in [12] is used. The Myint- Shinmura-Akaishi (MSA) potential [20] is applied for description of $\alpha\Lambda$ interaction. The results that correspond to the Isle potential [23] are shown in brackets. For $\alpha\alpha$ interaction the Ali-Bodmer potential of model "a" is chosen. The spin-orbit interaction is given by the S(M) potential.

| | J^π | Our | [12] |
|-------------------|---|-----------------|---------------|
| E_B | 1_1^+ | -6.559 (-6.674) | -6.61 (-6.63) |
| | 3_1^+ | -3.303 (-3.338) | - |
| | 5_1^+ | -3.368 (-3.409) | - |
| E_x ($ls) = 0$ | $(\frac{3}{2}^+ \text{ or } \frac{5}{2}^+)$ | 3.22 (3.30) | 3.19 (3.18) |

4. We have obtained some disagreement with the results of calculations [12] for the Isle potential (shown in brackets in Table 4). For MSA our result are close to one calculated in [12]. Note that the ($3/2^+$, $5/2^+$) excitation energy of the model [12] is slightly larger than the experimental value. We tested the S(M) potential, introduced above for spin-orbit interaction, in the framework of this model. Energy space for the ($3/2^+$, $5/2^+$) splitting (see Table. 4) is found to be about 70 eV. This value is larger than one obtained in our calculations for the ABe+TH(M)+S(MM) model and larger than the experimental value. However, one can generally conclude that the energies obtained within the Shoeb model correspond agreeably to the experimental data. At the same time we have to note that this result obtained by including into consideration the additional free parameters related to the three-body potential used. From our point of view such implementation is a weak point of the Shoeb model. We have shown that the experimental situation can be reproduced by our model while using only pair potentials. Final choice between both models one can perform on the basis of clear experimental indication of behavior of the $\alpha\Lambda$ potential at small distances. In the case of soft repulsive core potential the Shoeb model can be considered as appropriate. In the case of fully attractive $\alpha\Lambda$ potential this model can be considered as having extra free parameters.

5.4 Use of the ABe and TH(M) potentials in other cluster calculations

As shown above the cluster model with the ABe and TH(M) potentials can be successfully applied to reproduce spectral properties of the ${}^9_\Lambda\text{Be}$ hypernucleus. In this section we verify these inter-cluster potentials by applying them for other cluster systems. Two nuclei ${}^9\text{Be}$ and ${}^6_{\Lambda\Lambda}\text{He}$ (αn and $\alpha\Lambda\Lambda$, respectively) are appropriate examples of such cluster systems. The result for energy levels of the αn and $\alpha\Lambda\Lambda$ system obtained with the ABe and TH(M) potentials are presented in Tabl. 5. In these calculations the $\Lambda\Lambda$ semi-realistic potentials from Refs.[20, 34, 35] are used. The αn potential (FJR) is a modification of the Sack-Biedenharn-

Table 5. The ABe and TH(M) potentials are applied to estimate energy levels in the $\alpha\alpha n$ and $\alpha\Lambda\Lambda$ systems. All notations are the same as in Tabl. 1. The $\Lambda\Lambda$ semi-realistic potentials from Refs.[20,34,35] are used. The αn potential (FJR) is given in [37]. Experimental data are taken from [38] and [39].

| Nucl. | System | Pot. | J^π | Cal. | Exp. |
|----------------------------------|------------------------|------------------------------------|-----------------------|--------|------------|
| ${}^9\text{Be}$ | $\alpha\alpha n$ | FJR[37] | E_B $\frac{3}{2}^-$ | -1.863 | -1.576 |
| | | | E_x $\frac{5}{2}^-$ | 2.1(6) | 2.4294 |
| | | | E_x $\frac{1}{2}^-$ | 2.4(3) | 2.78 |
| | | | E_x $\frac{3}{2}^+$ | 2.8(3) | 3.049 |
| ${}^6_{\Lambda\Lambda}\text{He}$ | $\alpha\Lambda\Lambda$ | NSC97(b) NSC97(e) Myint [20] | E_B 0^+ | -6.43 | -7.25 |
| | | | | -6.80 | ± 0.19 |
| | | | | -7.04 | |
| | | | | | |

Breit potential (SBB) [36] taken from [37]. Presented results allow us to assert that the calculations with the ABe potential reliably reproduce the experimental spectral properties of the ${}^9\text{Be}$ nucleus. Obviously the calculated results depend also on the choice of αn potential. The use of the TH(M) potential in cluster calculations for ${}^6_{\Lambda\Lambda}\text{He}$ leads to weak binding of the $\alpha\Lambda\Lambda$ system if the known $\Lambda\Lambda$ potentials are used.

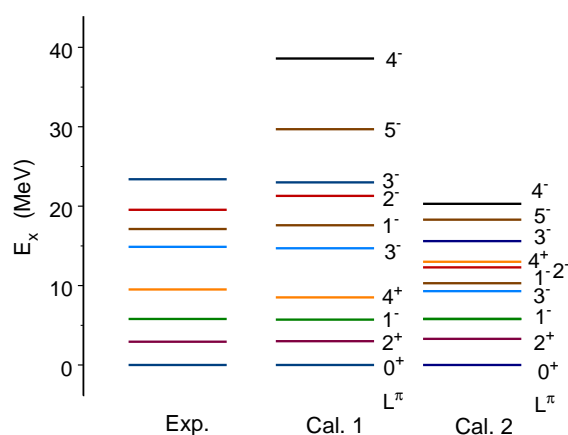


Fig. 1. Experimental (Exp.) and calculated (Cal.) spectrum of the ${}^9_{\Lambda}\text{Be}$. Cal.1 corresponds to our results. The results Cal.2 are from [16, 14]. Orbital momentum of each level is shown.

6 Summary

The configuration space Faddeev equations were applied to calculate the energy spectrum of the ${}^9_{\Lambda}\text{Be}$ hypernucleus within the $\alpha + \alpha + \Lambda$ cluster model. We found the set of phenomenological potentials that reproduces the ground state $\frac{1}{2}^+$ binding energy and excitation energy of the $\frac{5}{2}^+$ and $\frac{3}{2}^+$ states, simultaneously. In particular, the Ali-Bodmer potential of model "e" for $\alpha\alpha$ and modified Tang-Herdon potential for $\alpha\Lambda$ are used. The spin-orbit $\alpha\Lambda$ potential is

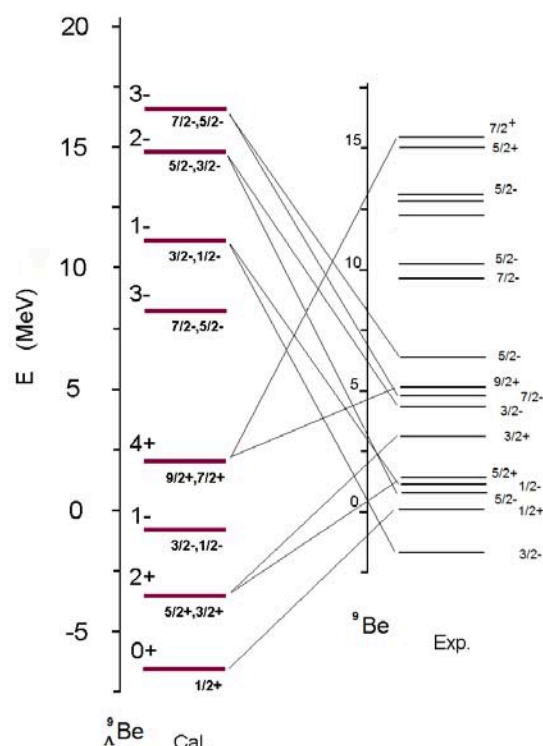


Fig. 2. Calculated (Cal.) and experimental (Exp.) spectrum of ${}^9\text{Be}$ and ${}^9_{\Lambda}\text{Be}$. The experimental data are from [16]. Orbital and total momentum of each level is shown. The levels with equal orbital momentum are connected by fine lines. Energy is measured from $\alpha + \alpha + \Lambda$ and $\alpha + \alpha + n$ thresholds, respectively.

described by modified Scheerbaum potential. Our calculations reproduce well the experimental data for excitation energies and therefore improve the previous cluster calculations for this hypernucleus. It is shown that the spectrum of ${}^9_{\Lambda}\text{Be}$ can be classified as an analog of the ${}^9\text{Be}$ spectrum with the exception of several "genuine hypernuclear states", which agrees qualitatively with previous studies. The energy spacing of spin-flip doublet ($\frac{9}{2}^+, \frac{7}{2}^+$) of about 200 keV is predicted by our model.

This work is supported by NSF CREST award HRD-0833184 and NASA award NNX09AV07A. The numerical calculations were performed at the Pittsburgh Supercomputing Center.

References

1. D.J. Millener, Nucl. Phys. **A804**, (2008) 84.
2. A. Gal, J.M. Soper, R.H. Dalitz, Ann. of Phys. **63**, (1971) 53; R.H. Dalitz, A. Gal, Phys. Rev. Lett. **36**, (1976) 362.
3. H. Bando, Nucl. Phys. **A450**, (1986) 217c.; H. Bando, T. Motoba, J. Zofka, Internat. J. Modern Phys. **21**, (1990) 4021.
4. E. Hiyama, M. Kamimura, T. Motoba, T. Yamada, Y. Yamamoto, Phys. Rev. **C66**, (2002) 024007.

5. Y. Fujiwara, M. Kohno, K. Miyagawa, Y. Suzuki, Phys. Rev. **C70**, (2004) 047002.
6. O. Portolho and S.A. Coon, J. Phys. G **17**, (1991) 375.
7. E. Hiyama, M. Kamimura, T. Motoba, T. Yamada, Y. Yamamoto, Prog. Theor. Phys. **C97**, (1997) 881.
8. S. Oryu, H. Kamada, H. Sekine, H. Yamashita, M. Nakazawa, Few-Body Systems **28**, (2000) 103.
9. E. Cravo, A.S. Fonseca, Y. Koike, Phys. Rev. **C66**, (2002) 014001-7.
10. I. Filikhin, A. Gal, V. M. Suslov, Nucl. Phys. **A743**, (2004) 194.
11. I. Filikhin, V.M. Suslov and B. Vlahovic, J. Phys. G: **30** (2004) 513.
12. M. Shoeb, Phys. Rev. **C74**, (2006) 064316.
13. T. Yamada, K. Ikeda, H. Bando, Prog. Theor. Phys. **73**, (1985) 397.
14. T. Yamada, K. Ikeda, T. Motoba, H. Bando, Phys. Rev. **C38**, (1988) 854.
15. I. Filikhin, V.M. Suslov and B. Vlahovic, Nucl. Phys. **A 790**, (2007) 695; arXiv:nucl-th/0610096.
16. O. Hashimoto, H. Tamura, Progress in Particle and Nuclear Physics **57**, (2006) 564.
17. L.D. Faddeev and S.P. Merkuriev, *Quantum Scattering Theory for Several Particle Systems* (Kluwer Academic, Dordrecht 1993) pp. 398.
18. S. Ali and A.R. Bodmer, Nucl. Phys. **80**, (1966) 99.
19. Y.C. Tang, R.C. Herndon, Phys. Rev. **B138**, (1965) 637; R.H. Dalitz, B.W. Downs, Phys. Rev. **111**, (1958) 967.
20. K. S. Myint, S. Shinmura and Y. Akaishi, Eur. Phys. J. **A16** (2003), 21.
21. D.J. Millener, Nucl. Phys. **A754**, (2005) 48c.
22. C. Daskaloyannis, M. Grypeos, H. Nassena, Phys. Rev. **C26**, (1982) 702
23. Y. Kurihara, Y. Akaishi, H. Tanaka, Phys. Rev. **C84**, 971 (1985).
24. Y. Fujiwara, M. Kohno, Y. Suzuki, Mod. Phys. Lett. **A24**, (2009) 1031.
25. J. Bernabeu, V.M. Suslov, T.A. Strizh, S.I. Vinitzky, Hyperfine Interaction, **101/102**, (1996) 391.
26. H. Akikawa et al., Phys. Rev. Lett., **88**, (2002) 082501-1; H. Tamura, Nucl. Phys. **A754**, (2005) 58c.
27. V. I. Kukulin, V. M. Krasnopolsky and J. Horacek, *Theory of Resonances* (Kluwer, Dordrecht 1989).
28. C. Kurokawa and K. Kato, Phys. Rev. **C76**, (2005) 021301-1.
29. I. Filikhin, V.M. Suslov and B. Vlahovic, J. Phys. G **31**, (2005) 1207.
30. I. Filikhin, V.M. Suslov and B. Vlahovic, Phys. Atom. Nucl. **72**, (2009) 619.
31. D.V. Fedorov, A.S. Jensen, Phys. Lett. **B389**, (1996) 631.
32. M. Juric et al., Nucl. Phys. **B52**, (1973) 1.
33. M. Shoeb and Sonika, Phys. Rev. **C 79**, (2009) 054321.
34. I. N. Filikhin and A. Gal, Nucl. Phys. **A707**, (2002) 491.
35. I.N. Filikhin, A. Gal, V.M. Suslov Phys. Rev. **C68**, (2003) 024002.
36. S. Sack, L.C. Biedenharn, G. Bret, Phys. Rev. **93**, (1954) 321.
37. D.V. Fedorov, A.S. Jensen, and K. Riisager, Phys. Rev. **C49**, (1994) 201; A. Cobis, D.V. Fedorov and A.S. Jensen, Nucl. Phys. **A631**, (1998) 793.
38. Nuclear data evaluation project, <http://www.tunl.duke.edu/nucldata/>
39. H. Takahashi et al., Phys. Rev. Lett. **87** (2001) 212502.